

Effect of Surface Deposits on Electromagnetic Waves Propagating in Uniform Ducts

Kenneth J. Baumeister
Lewis Research Center
Cleveland, Ohio

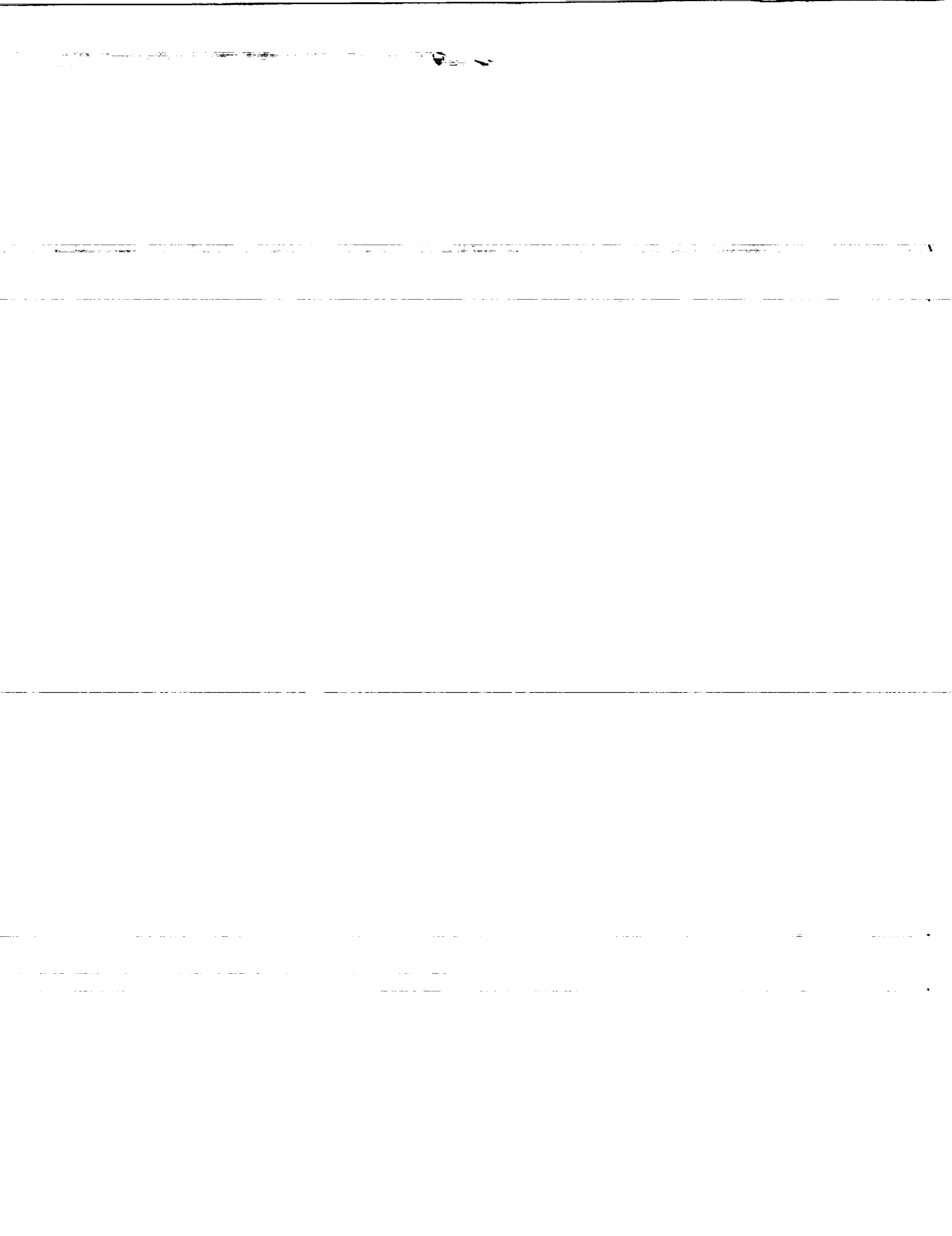
(NASA-TM-103282) EFFECT OF SURFACE DEPOSITS
ON ELECTROMAGNETIC WAVES PROPAGATING IN
UNIFORM DUCTS (NASA) 13 p CSCL 20N

N91-10208

Unclas
63/32 0310595

Prepared for the
Fourth Biennial IEEE Conference on Electromagnetic Field Computation
Toronto, Ontario, October 22-24, 1990

NASA



EFFECT OF SURFACE DEPOSITS ON ELECTROMAGNETIC WAVES PROPAGATING
IN UNIFORM DUCTS

Kenneth J. Baumeister
National Aeronautics and Space Administration
Lewis Research Center
Cleveland, Ohio 44135

SUMMARY

E-5737 A finite-element Galerkin formulation has been used to study the effect of material surface deposits on the reflective characteristics of straight uniform ducts with PEC (perfectly electric conducting) walls. Over a wide frequency range, the effect of both single and multiple surface deposits on the duct reflection coefficient were examined. The power reflection coefficient was found to be significantly increased by the addition of deposits on the wall.

INTRODUCTION

Many common waveguide components are intrinsically mismatched. The mismatch is often corrected by placing a discontinuity (deposit) or so called iris into a duct or guide to correct the problem (Alison, 1972, p. 137). Marcuvitz (1986) has presented analytical models which describe the effects of many discontinuities on microwave networks. He presents equivalent-circuit parameters in both analytical and graphical numerical form which allow predictions of the scattering properties of the discontinuity. The predictions apply to metallic discontinuities where the wavelength is generally much larger than the discontinuity.

In the present paper, a finite-element Galerkin formulation has been used to study the effect of material deposits on the reflective characteristics of a two-dimensional straight uniform duct. The present work will broaden previous work to include dielectric deposits and to wavelengths on the order of the size of the deposits. This paper will focus on the interaction of a plane propagating TM duct mode traveling down the uniform entrance duct with both single and multiple two-dimensional material rivulet deposited on the lower wall as shown in figure 1.

In a number of case studies, the effect of material deposit length, width and excitation frequency on the power reflection coefficient will be examined.

NOMENCLATURE

- b'_a characteristic duct height
 b_a dimensionless entrance height $b'_a/b_a = 1$
 c'_0 speed of light in vacuum

- f dimensionless frequency of waves, equation (7)
- g distance gap between deposits
- H'_0 normalizing magnitude of magnetic intensity
- H'_x x component of magnetic intensity of waves, H'_x/H'_0
- \tilde{H}_x finite-element approximation to H_x
- h height of material rivulet deposit
- j $\sqrt{-1}$
- L dimensionless length, L'/b'_a
- n integer
- P_0 input energy in positive x direction
- P_z reflected energy in negative z direction
- t dimensionless time, $\frac{c'_0}{b'_a} t'$
- w width of material rivulet deposit, w'/b'_a
- x dimensionless transverse distance, x'/b'_a
- y dimensionless transverse distance, y'/b'_a
- z dimensionless axial distance, z'/b'_a
- ϵ total complex permittivity, equation (4)
- ϵ' permittivity
- ϵ_a dielectric constant in entrance duct, ϵ'_a/ϵ'_0
- ϵ'_0 permittivity in vacuum
- ϵ_r complex dielectric constant, ϵ'/ϵ'_0
- ϵ_r^I imaginary part of dielectric constant

ϵ_T^I total imaginary part of permittivity, equation (4)

ϵ_r^R real part of dielectric constant

λ wavelength

μ total permeability, equation (5)

μ' permeability

μ'_0 permeability in vacuum

μ_r relative permeability, μ'/μ'_0

μ_r^I imaginary part of relative permeability

μ_r^R real part of relative permeability

σ dimensionless conductance, $\frac{\sigma' b'_a}{c'_0 \epsilon'_0}$

ω' angular velocity

ω dimensionless angular velocity, $\frac{\omega' b'_a}{c'_0}$

Subscripts:

a entrance region

o reference value (entrance region)

Superscripts:

' dimensional quantity

~ approximate quantity

GOVERNING EQUATION AND BOUNDARY CONDITIONS

The dimensionless duct coordinates used to describe the duct in figure 1 are defined as

$$y = \frac{y'}{b'_a} \quad z = \frac{z'}{b'_a} \quad L = \frac{L'}{b'_a} \quad b_a = \frac{b'_a}{b'_a} = 1 \quad (1)$$

with b'_a the height of the duct used as the characteristic length in converting to dimensionless quantities. The prime, ', is used to denote a dimensional quantity and the unprimed symbols define a dimensionless quantity. This convention will be used throughout this report. These and all other symbols used in the report are defined in the nomenclature.

For time harmonic variations in the electromagnetic field

$$\text{Magnetic intensity} = H_x(y,z)e^{+j\omega t} \quad (2)$$

The governing differential equations are the standard Maxwell's equations which can be combined to form a single variable property wave equation for the transverse magnetic wave propagation (Silvester, 1983, p. 48, eq. (4.07)). For a two-dimensional duct, the scalar form of the wave equation can be written as (Baumeister, 1986, eq. (25))

$$\frac{\partial}{\partial y} \left(\frac{1}{\epsilon} \frac{\partial H_x}{\partial y} \right) + \frac{\partial}{\partial z} \left(\frac{1}{\epsilon} \frac{\partial H_x}{\partial z} \right) + \omega^2 \mu H_x = 0 \quad (3)$$

where the total permittivity including conduction, and the total permeability are defined as

$$\epsilon = \epsilon_R^R - j \left(\epsilon_R^I + \frac{\sigma}{\omega} \right) = \epsilon_R^R - j \epsilon_T^I \quad (4)$$

$$\mu = \mu_R^R - j \mu_T^I \quad (5)$$

(Cheng, p. 300 or Harrington, pp. 24 and 25, equations (1-74), (1-76) and (1-77)). The various parameters are real positive quantities with dimensionless conductivity,

$$\sigma = \frac{\sigma' b'_a}{c'_0 \epsilon'_0} \quad (6)$$

dimensionless frequency f

$$f = \frac{f' b'_a}{c'_0} = \frac{b'_a}{\lambda'_0} \quad (7)$$

and

$$\omega = 2\pi f \quad (8)$$

A variety of boundary conditions will be used in the finite-element solution of equation (3). Each of the required conditions will now be briefly discussed.

A modal solution (Cheng, 1983, p. 458) is used to represent the magnetic field in the semi-infinite, PEC wall entrance and exit regions while a finite element solution is used to generate the solution in the portion of the duct

containing the material deposit. The elements representing the material deposits inside the air duct require no special consideration such as an interfacial boundary condition. The heterogeneous form of the wave equation, equation (3), automatically handles the change in properties.

Continuity of the tangential components of the magnetic and electric field is applied at the entrance and exit interfaces separating the finite element and modal regions (Baumeister, 1986). The analysis also assumes a given number of propagating modes moving down the entrance duct towards the material deposits embedded in the finite element region. These modes effectively set the level of the magnetic field in the finite element region.

At the perfectly conducting wall surrounding the duct, the tangential component of the electric field vector is zero (Cheng, 1983, eq. (7-52(a)) or Kraichman, 1970, eq. (1.69)). Again, using Maxwell's equations to relate the electric field to the magnetic field (Jordan, 1968, eq. (7-4)), the component of the gradient of the magnetic field normal to the perfectly conducting walls shown in figure 2 becomes

$$\nabla_{\tilde{H}_x} \cdot \bar{n} = 0 \quad (9)$$

FINITE ELEMENT THEORY

In the central portion of the duct used to contain the material deposits, the continuous domain is first divided into a number of discrete triangular areas as shown in figure 2. The magnetic field will be determined at the nodes which define the corners of the triangles. The finite element aspects of converting equation (3) and the boundary conditions into an appropriate set of global difference equations can be found in text books (Burnett, 1987) or more explicitly in the paper presented by Baumeister (1986) and for conciseness will not be presented herein.

In the finite element region, electromagnetic properties are assigned to each element represent by a small triangle shown in figure 2. In most cases, the values of ϵ and μ are assigned values of unity associated with air properties. However, those elements which are forced to align with the material deposits can have an assigned real value of ϵ ranging from 3.0 to 9.0. The value of the permeability remains at unity.

RESULTS AND COMPARISONS

A number of example calculations are now presented to calculate the reflected energy coefficient of a plane TM wave propagating down the uniform ducts shown in figure 1 with a material deposit on the wall. The reflection coefficient in decibels is defined as

$$\text{dB} = 10 \log_{10} \left[\frac{P_z}{P_o} \right] \quad (10)$$

where P_o is the propagating input energy in the positive z direction and P_z is the reflected propagating energy in the negative z direction. The

energy is a product of the magnetic and electric fields (Poynting Vector) and duct area as presented by Baumeister (1986, eqs. (86) and 88)). Material deposits of heights and widths of 10 and 5 percent of the duct height were considered in the calculations to follow. The range of dimensionless frequencies (eq. (7)) calculated will be from 0.5 to 5.

Example 1: Reflection Coefficient As Function of Frequency

The reflected power coefficient for a single two-dimensional material deposit of 0.1 height and width is shown in figure 3. The geometrical configuration is shown by the inserted sketch. The lowest solid line defined by the o symbols represents the reflective power from the duct without deposits. It should be at minus infinity because in principle no reflection should occur in the straight duct. The approximately 60 dB down curve solely represents numerical inaccuracies in the calculation.

As seen in figure 3, the material deposit significantly increases the total reflective power over a wide frequency range as compared to a duct without deposits. To generate figure 3, 37 nodes are used in the transverse y direction and 60 nodes in the axial z direction. The reflection coefficients displayed in figure 3 have considerable scatter at the higher frequencies. To check on numerical convergence, the calculation was repeated with 49 nodes in the y direction and the same number of nodes per wavelength in the axial z direction. As seen in figure 4 the onset of scatter in the reflection coefficient still begins at a dimensionless frequency of 1.5 which is the same scattering onset frequency seen in figure 3. Also, the magnitude of the reflection coefficients are in agreement in both figures 3 and 4. Therefore, both calculations have converged to the same results. The physical nature of this high frequency fluctuation in the reflection coefficient will be discussed shortly. Similar results are also shown in figure 5, for a deposit of 0.05 height and width. In this case the reflection coefficient are lower than those shown in figure 3 due to the reduction in cross section area of the deposit. As expected, for both the 0.1 and 0.05 deposits, the reflection coefficient decreases at the lower frequencies. In the lower frequency cases, the diffusive nature of the electromagnetic wave allows the energy to bend around the obstructions in the duct and thereby reduce the reflection coefficient.

As seen in figures 3 to 5, as the frequency increases the various material curves begin to overlap. In figure 4, overlapping of the reflection coefficient begins at a dimensionless frequency of 1.5 for a deposit height and width of 0.1 while the overlapping begins at a dimensionless frequency of 3.0 for the deposit of 0.05 height and width as shown in figure 5. The scatter of the reflection coefficient at these higher frequencies appears to be a direct result of periodic impedance matching of the signal and the material deposits. This scattering phenomena can be related to the standard radome design calculation. For a dielectric window as shown in figure 6, the absence of reflections occurs for the thinnest radome when the following dimensions occur.

$$w' = \frac{\lambda_2'}{2} = \frac{1}{2f' \sqrt{\mu_2' \epsilon_2'}} = \frac{c_0'}{2f' \sqrt{\mu_2 \epsilon_2}} \quad (11)$$

(Cheng 1983, p. 351)

Dividing both sides of equation (11) by the characteristic duct height b'_a and setting μ equal to 1 yields (assume $\epsilon_{r1} = 1$ and $\epsilon_{r2} = \epsilon_r$)

$$w = \frac{1}{2f\sqrt{\epsilon_r^R}} \quad (12)$$

Or, the frequency associated with zero reflection

$$f = \frac{1}{2w\sqrt{\epsilon_r^R}} \quad (13)$$

For example, in figure 4 if

$$w = 0.1 \quad \epsilon_r^R = 9.0 \quad (14)$$

then f according to equation (13) has a value of 1.66. This corresponds to the first crossover point in figure 4. According to equation (13) the crossovers for the smaller values of the relative permittivity occur at higher frequencies as is seen in figures 3 and 4. For example, for a permittivity of 5.0, equation (13) predicts a crossover frequency of 2.23 which corresponds to the results shown in figure 4. For the thinner deposit of 0.05 the predicted f value from equation (13) will double to 3.3. This agrees with the finite element results in figure 5 where the crossover is now delayed till a frequency of 3.0.

Equation (13) can be written in its more general form as

$$f = \frac{n}{2w\sqrt{\epsilon_r^R}} \quad (15)$$

where n is an integer (Cheng 1983, p. 351). The higher values of n account for the continued fluctuations in the reflection curves as the frequency increases.

Example 2: Reflection Coefficients As Function of Deposit Height

Similarly, for material deposits of 0.05 and 0.1 height and width, the relationship in reflected power with deposit height is shown in figure 7. Again, the geometrical configuration is shown by the inserted sketch. With normal plane wave incidence, the reflection coefficient can be roughly estimated by the simple formula

$$\text{dB} = 20 \log_{10} \left[\frac{h_i}{b_a} \right] \quad (16)$$

This formula assumes all normally directed rays which contact the material deposit are reflected. For a deposit to duct height ratio of 0.1, equation (16) predicts -20 dB which is close to the calculated value calculated by the finite element theory at the higher frequencies shown in figure 7. Similarly, when the deposit to duct height ratio is 0.05, equation (16) gives rise to a 6 dB lower value of -26 dB which again is close to the finite element prediction shown in figure 7.

Example 3: Reflection Coefficient for Multiple Deposits

Finally, for two deposits of 0.1 in height and width placed in a uniform duct, the relationship in the reflection coefficient and the gap between the deposits is shown in figure 8. Again, the geometrical configuration is shown by the inserted sketch. The circular symbol represents the smooth duct while the square symbol with the dashed connecting lines represents a single deposit.

Generally, the two deposits have a slightly higher reflection coefficient than the single deposit. There does not seem to be any obvious trends with the gap thickness between the deposits. At dimensionless frequencies below 1.5, however, the reflection coefficient for the two deposits can drop below the value for the single deposit. This may be the result of some impedance matching as was discussed earlier.

CONCLUDING REMARKS

A finite-element electromagnetic duct propagation code was modified to study transverse magnetic (TM) wave propagation in two-dimensional uniform ducts with material deposits on the walls. Example solutions illustrated the relationship of material deposit length, width and excitation frequency on the power reflection coefficient of the duct. Small single two-dimensional material rivulet deposits were found to significantly increase the reflected energy.

REFERENCES

- Alison, W.B.W.: A Handbook for the Mechanical Tolerancing of Waveguide Components, Artech House, 1987.
- Baumeister, K.J.: Finite Element Analysis of Electromagnetic Propagation in an Absorbing Wave Guide. NASA TM-88866, 1986.
- Burnett, D.S.: Finite Element Analysis: From Concepts to Applications. Addison-Wesley, Reading, MA, 1987.
- Cheng, D.K.: Field and Wave Electromagnetics. Addison-Wesley, Reading, MA, 1983.
- Harrington, R.F.: Time-Harmonic Electromagnetic Fields. McGraw-Hill, 1961.
- Jordan, E.C.; and Balmain, K.G.: Electromagnetic Waves and Radiating Systems. 2nd ed., Prentice-Hall, 1968.

Kraichman, M.B.: Handbook of Electromatic Propagation in Conducting Media. NAVMAT P-2302, U.S. Government Printing Office, Washington, D.C., 1970.

Marcuvitz, N.: Waveguide Handbook. Peter Peregrinus Ltd., 1986.

Silvester, P.P.; and Ferrari, R.L.: Finite Elements For Electrical Engineers. Cambridge University Press, 1983.

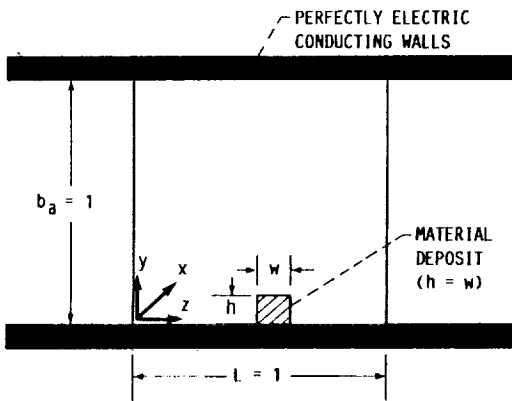


FIGURE 1. - DUCT GEOMETRY AND COORDINATE SYSTEM.

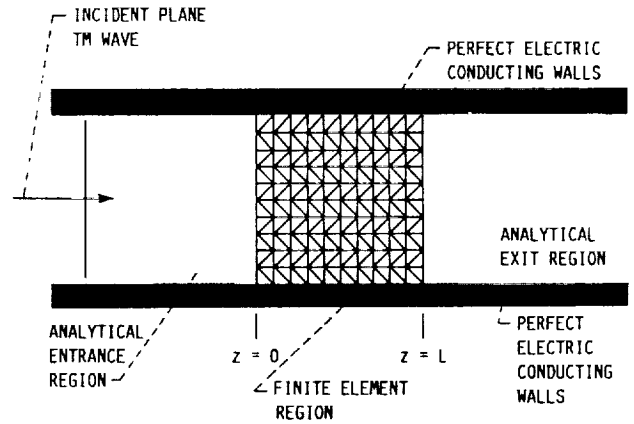


FIGURE 2. - TWO DIMENSIONAL UNIFORM DUCT FINITE ELEMENT MODEL.

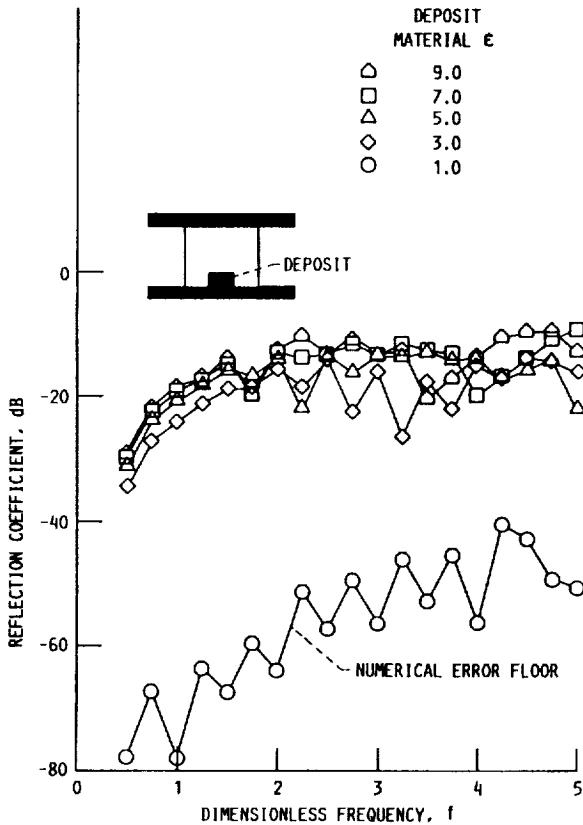


FIGURE 3. - ENERGY REFLECTION COEFFICIENT OF A SINGLE DEPOSIT ($h = w = 0.1$) FOR A PLANE TM WAVE INCIDENT AS A FUNCTION OF FREQUENCY.

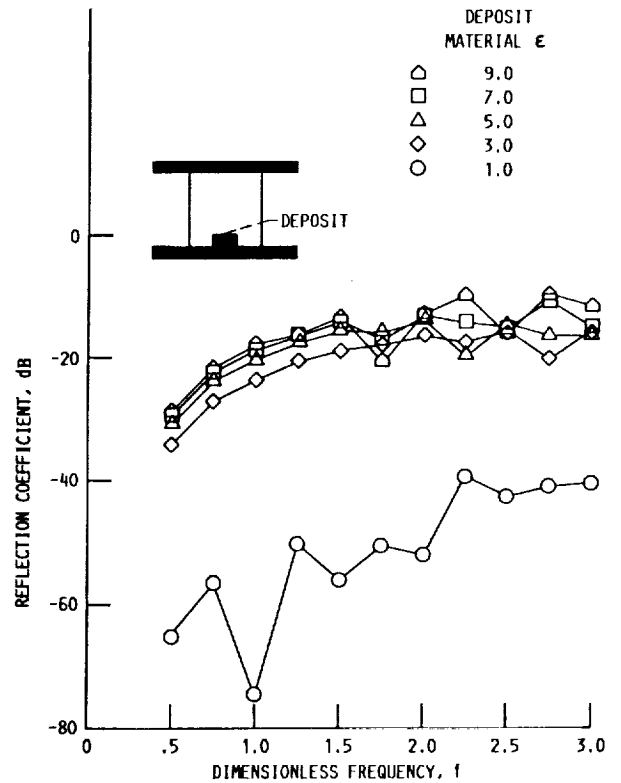


FIGURE 4. - ENERGY REFLECTION COEFFICIENT OF A SINGLE DEPOSIT ($h = w = 0.1$) FOR A PLANE TM WAVE INCIDENT AS A FUNCTION OF FREQUENCY WITH 49 TRANSVERSE GRID MODES.

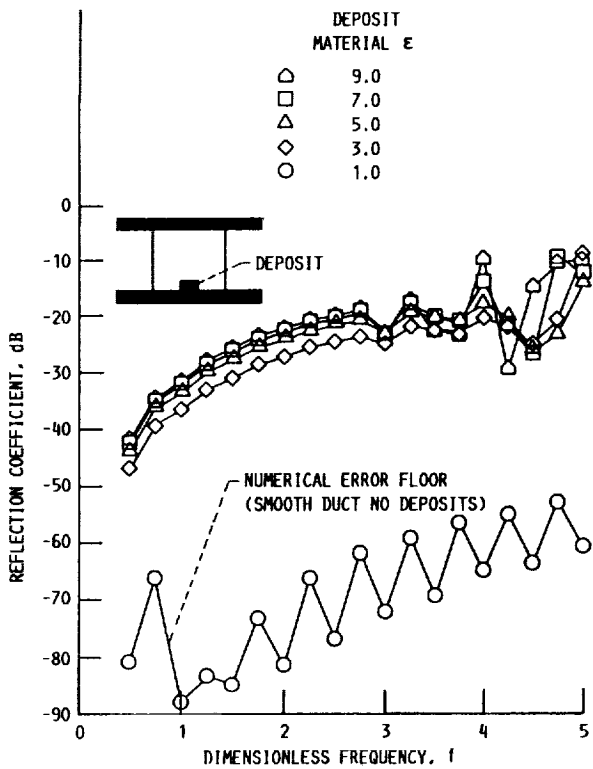


FIGURE 5. - ENERGY REFLECTION COEFFICIENT OF A SINGLE DEPOSIT ($h = w = 0.05$) FOR AN INCIDENT PLANE TM WAVE AS A FUNCTION OF FREQUENCY.

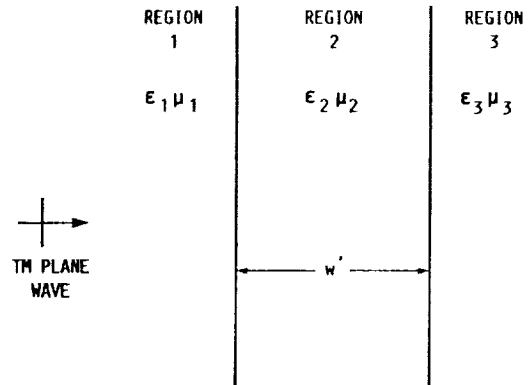


FIGURE 6. - RADOME GEOMETRY FOR PLANE WAVE INCIDENCE.

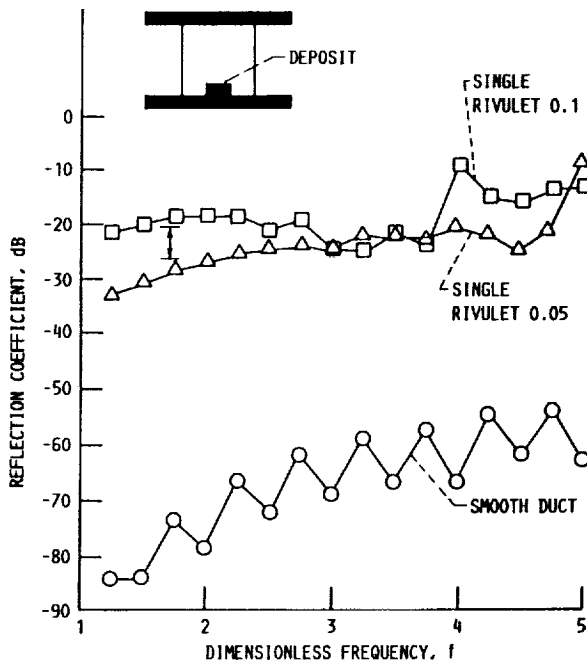


FIGURE 7. - ENERGY REFLECTION COEFFICIENT OF UNIFORM DUCT WITH ($\epsilon = 3.0$) RIVULET FOR PLANE WAVE INCIDENCE AS A FUNCTION OF FREQUENCY.

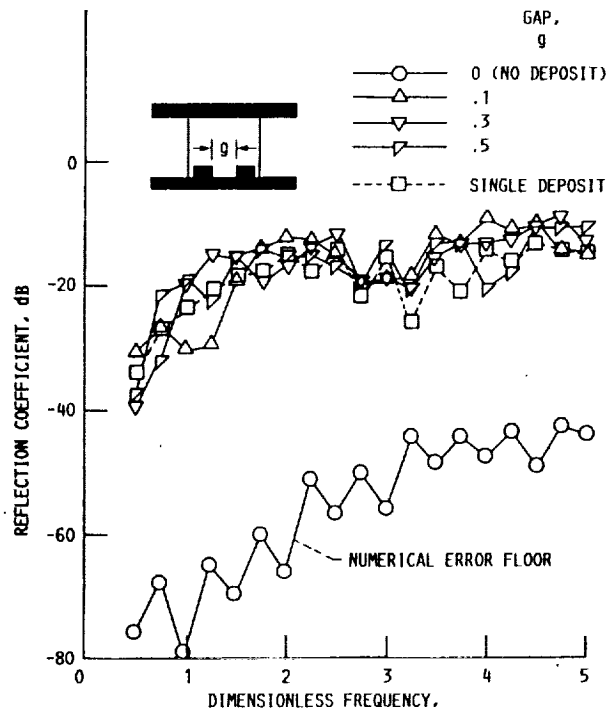


FIGURE 8. - ENERGY REFLECTION COEFFICIENT OF TWO DEPOSITS FOR PLANE TM WAVE INCIDENT AS A FUNCTION OF GAP BETWEEN THE DEPOSITS ($h = w = 0.1$) AND $\epsilon = 3.0$.



National Aeronautics and
Space Administration

Report Documentation Page

1. Report No. NASA TM-103282		2. Government Accession No.		3. Recipient's Catalog No.	
4. Title and Subtitle Effect of Surface Deposits on Electromagnetic Waves Propagating in Uniform Ducts				5. Report Date	
				6. Performing Organization Code	
7. Author(s) Kenneth J. Baumeister				8. Performing Organization Report No. E-5737	
				10. Work Unit No. 505-62-21	
9. Performing Organization Name and Address National Aeronautics and Space Administration Lewis Research Center Cleveland, Ohio 44135-3191				11. Contract or Grant No.	
				13. Type of Report and Period Covered Technical Memorandum	
12. Sponsoring Agency Name and Address National Aeronautics and Space Administration Washington, D.C. 20546-0001				14. Sponsoring Agency Code	
15. Supplementary Notes Prepared for the Fourth Biennial IEEE Conference on Electromagnetic Field Computation, Toronto, Ontario, October 22-24, 1990.					
16. Abstract A finite-element Galerkin formulation has been used to study the effect of material surface deposits on the reflective characteristics of straight uniform ducts with PEC (perfectly electric conducting) walls. Over a wide frequency range, the effect of both single and multiple surface deposits on the duct reflection coefficient were examined. The power reflection coefficient was found to be significantly increased by the addition of deposits on the wall.					
17. Key Words (Suggested by Author(s)) Electromagnetics Duct Deposits Finite elements			18. Distribution Statement Unclassified - Unlimited Subject Category 32		
19. Security Classif. (of this report) Unclassified		20. Security Classif. (of this page) Unclassified		21. No. of pages 12	22. Price* A03

